# SCIENTIFIC REPORT

## “Integrated radiating focusing systems: full-wave modeling of SIW beamformers and antennas”

**Casaletti Massimiliano, NEWFOCUS grant n. 3677**

## Purpose of the visit

The major objective of the work was to develop an efficient full wave numerical code for the analysis of SIW focusing beamforming networks and beam scanning antennas. Substrate Integrated Waveguides (SIW) structures are realized using standard printed circuit board (PCB) technology which is easy and cheap to produce. The basic idea is to realize waveguide channels on a grounded dielectric slab by using arrays of metallic vias.
The focus of the work has been the analysis of integrated reflectors used as quasi-optical beamformers for multiple beam antennas at millimeter waves. More precisely, the generic antenna configuration that is selected is the so-called pillbox antennas recently patented by IETR. The pillbox antennas (Fig. 1a) are very attractive since they provide excellent scanning performance (Fig. 1b).
The design of these quasi-optical systems (electrically very large structures) can be extremely time consuming and memory demanding.

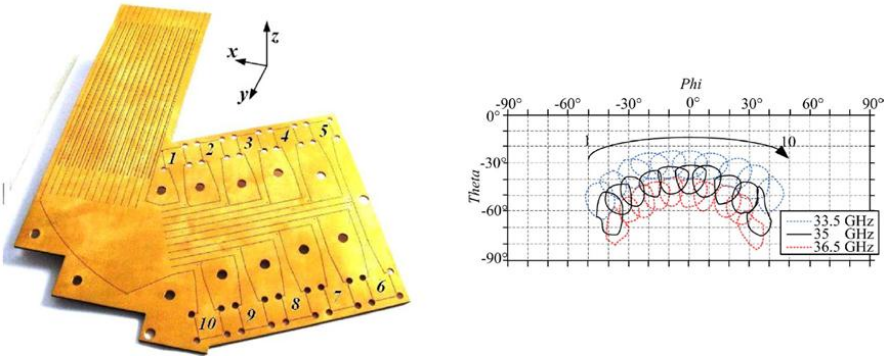


(a) 2D beam scanning SIW antenna. Here the quasi-optical system is an integrated offset reflector

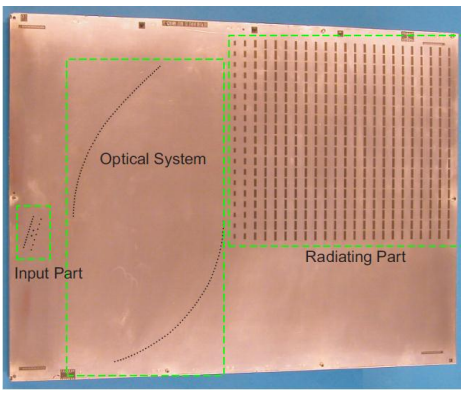


(b) Single-beam SIW antenna with an integrated double-reflector focusing system

Fig. 1. Examples of multiple beam antennas with an integrated SIW focusing system used as a beamformer.

## Description of the work carried out during the visit

The analysis of large structures consisting of conventional waveguides found in literature has been performed in an efficient way by using the method of the moments, thanks to the availability of the waveguide Green's function.
Following the same principle we have introduced a new semi-analytical Green's function for the SIW waveguides. Then, using the equivalence principle the whole structure has been decomposed into a set of SIW waveguides coupled through equivalent magnetic sources. Finally this simplified problem was analyzed by a method of the moment technique making use of the above mentioned SIW waveguide Green's function.

The work has been divided into two successive steps:
1. Derivation of the Green's function for an SIW waveguide.
2. Efficient evaluation of the radiated field by an SIW pillbox antenna.

### *1. Green's function for a SIW waveguide*

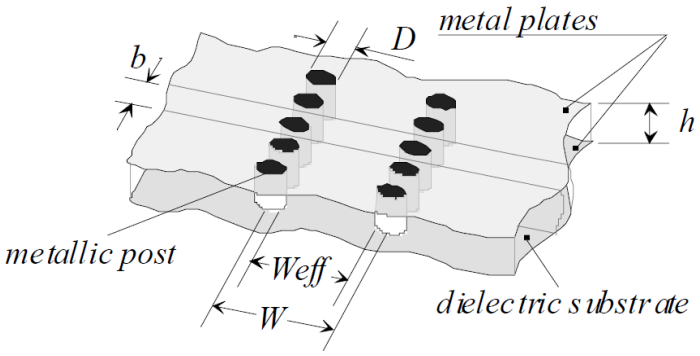


**Fig. 2.** Topology of an SIW guide realized on a dielectric substrate with its physical dimensions.

The SIW waveguide (Figure 2) is modelled as an ensemble of cylindrical scatterers used to design waveguides, reflectors, feeder, etc., inside a Parallel Plate Waveguides (PPW) fed by magnetic currents.
The field inside the waveguide structure has been decomposed as the superposition of an incident field (the field radiated by the sources in the homogeneous PPW) and the field scattered by the dielectric or metallic posts

$$\underline{\underline{\mathbf{G}}} = \underline{\underline{\mathbf{G}}}_{inc} + \underline{\underline{\mathbf{G}}}_{s} . \tag{1}$$

Since all the scatterers have cylindrical shape the incident and scattered fields have been expanded as a cylindrical wave vectors expansion. This allows us to easily impose the boundary condition on every cylinder since every component of the incident field was conformal to the scatterer surfaces.

The dyadic Green's function for the incident magnetic field radiated by a magnetic source $\mathbf{M}_s$ is given by

$$\underline{\underline{\mathbf{G}}}_{inc} = \underline{\underline{\mathbf{G}}}^{(1)}\left(\mathbf{r},\mathbf{r}'\right) \tag{2}$$

where $\underline{\underline{\mathbf{G}}}^{(1)}$ is the dyadic Green's function for a PPW, $\mathbf{r}$ is the observation point and $\mathbf{r}'$ is the source position.

Following the procedure introduced by Felsen and Marcuvitz, the primary dyadic $\underline{\underline{\mathbf{G}}}^{(1)}$ Green's function for a PPW can be obtained in symmetric form with respect to source and observation positions from two scalar TM ($\ell'$) and TE ($\ell''$) potentials

$$-j\omega\mu\underline{\underline{\mathbf{G}}}^{(1)}(\mathbf{r},\mathbf{r}') = k^2(\nabla\times\hat{\mathbf{z}})(\nabla'\times\hat{\mathbf{z}})\ell'(\mathbf{r},\mathbf{r}') + (\nabla\times\nabla\times\hat{\mathbf{z}})(\nabla'\times\nabla'\times\hat{\mathbf{z}})\ell''(\mathbf{r},\mathbf{r}') - \left(\hat{\mathbf{z}}\hat{\mathbf{z}} + \frac{\nabla_t\nabla_t}{\nabla_t^2}\right)\delta(\mathbf{r}-\mathbf{r}') \tag{3}$$

where $k = \omega\sqrt{\varepsilon\mu}$, $\nabla$ and $\nabla'$ denote the gradient operator with respect to the observation and source coordinates respectively, and $\nabla_t = \nabla - \frac{\partial}{\partial z}\hat{\mathbf{z}}$ represents the transverse nabla operator.

Using representation (3) with a transmission line radial equation method lead to the final expression

$$\begin{aligned}\underline{\underline{\mathbf{G}}}^{(1)}(\mathbf{r},\mathbf{r}') = &-\frac{1}{k^2}\left(\hat{\mathbf{z}}\hat{\mathbf{z}} + \frac{\nabla_t\nabla_t}{\nabla_t^2}\right)\delta(\mathbf{r}-\mathbf{r}') - j\sum_{m=0}^{+\infty}\sum_{n=-\infty}^{\infty}(-1)^n\left(1-\frac{\delta_{m0}}{2}\right)\frac{1}{2k_{\rho_m}^2 h}\Big[\mathbf{M}_n\left(k_{\rho_m},k_{z_m},\boldsymbol{\rho},z\right)\mathbf{M}_n'\left(k_{\rho_m},k_{z_m},\boldsymbol{\rho}',z'\right)\\ &+\mathbf{N}_n\left(k_{\rho_m},k_{z_m},\boldsymbol{\rho},z\right)\mathbf{N}_n'\left(k_{\rho_m},k_{z_m},\boldsymbol{\rho}',z'\right) + (\nabla\times\hat{\mathbf{z}})(\nabla'\times\hat{\mathbf{z}})\frac{4j\delta(\boldsymbol{\rho}-\boldsymbol{\rho}')}{\nabla_t^2}\cos\left(k_{z_m}z\right)\cos\left(k_{z_m}z'\right)\\ &+\frac{(\nabla\times\nabla\times\hat{\mathbf{z}})(\nabla'\times\nabla'\times\hat{\mathbf{z}})}{k^2}\frac{4j\delta(\boldsymbol{\rho}-\boldsymbol{\rho}')}{\nabla_t^2}\sin\left(k_{z_m}z\right)\sin\left(k_{z_m}z'\right)\Big]\end{aligned} \tag{4}$$

where $k_{\rho_m} = \sqrt{k^2 - k_{z_m}{}^2}$, $k_{z_m} = \frac{m\pi}{h}$, $\delta_{m0}$ is the Kronecker's delta function, $\mathrm{H}_n^{(2)}$ is the *n*-th order Hankel function of second kind, *m* and *n* are the mode indexes along *z* and *φ* directions, respectively and $\mathbf{M}_n, \mathbf{N}_n$ are cylindrical vectors eigenfunctions defined as

$$\begin{aligned}\mathbf{M}_n &= \begin{cases}\nabla\times\hat{\mathbf{z}}\,\mathrm{H}_n^{(2)}\left(k_{\rho_m}\rho\right)e^{-jn\phi}\cos\left(k_{z_m}z\right) & \rho > \rho'\\ \nabla\times\hat{\mathbf{z}}\,\mathrm{J}_n\left(k_{\rho_m}\rho\right)e^{-jn\phi}\cos\left(k_{z_m}z\right) & \rho \le \rho'\end{cases}\\ \mathbf{N}_n &= \begin{cases}\frac{1}{k}\nabla\times\nabla\times\hat{\mathbf{z}}\,\mathrm{H}_n^{(2)}\left(k_{\rho_m}\rho\right)e^{-jn\phi}\sin\left(k_{z_m}z\right) & \rho > \rho'\\ \frac{1}{k}\nabla\times\nabla\times\hat{\mathbf{z}}\,\mathrm{J}_n\left(k_{\rho_m}\rho\right)e^{-jn\phi}\sin\left(k_{z_m}z\right) & \rho \le \rho'\end{cases}\end{aligned} \tag{5}$$

$\mathbf{M}'_n, \mathbf{N}'_n$ can be obtained from (5) by inverting $\rho > \rho'$ with $\rho \le \rho'$.

The magnetic field scattered by each post $\underline{\underline{\mathbf{G}}}_s$ is expressed as a linear combination of transverse (with respect to *z*) magnetic ($\mathrm{TM}_z$) and electric ($\mathrm{TE}_z$) outgoing CVW satisfying the boundary conditions on the metallic plates

$$\mathbf{G}_s(\mathbf{r}) = \sum_{p=1}^{N_{post}} \sum_{m=1}^{+\infty} \sum_{n=-\infty}^{+\infty} A_{m,n,p}^{TM} \mathbf{M}_n\left(k_{\rho_m}, k_{z_m}, \boldsymbol{\rho}-\boldsymbol{\rho}_p, z\right) + A_{m,n,p}^{TE} \mathbf{N}_n\left(k_{\rho_m}, k_{z_m}, \boldsymbol{\rho}-\boldsymbol{\rho}_p, z\right) \quad (6)$$

where

$$\mathbf{M}_n = \nabla \times \left[\hat{\mathbf{z}}\, \mathrm{H}_n^{(2)}\left(k_{\rho_m}\rho\right) e^{-jn\phi} \cos\left(k_{z_m} z\right)\right], \quad \mathbf{N}_n = \frac{1}{k} \nabla \times \nabla \times \left[\hat{\mathbf{z}}\, \mathrm{H}_n^{(2)}\left(k_{\rho_m}\rho\right) e^{-jn\phi} \sin\left(k_{z_m} z\right)\right] \quad (7)$$

The unknown scattered field coefficients $A_{m,n,p}^{TM}$ and $A_{m,n,p}^{TE}$ are derived by imposing the boundary conditions on the post surfaces.

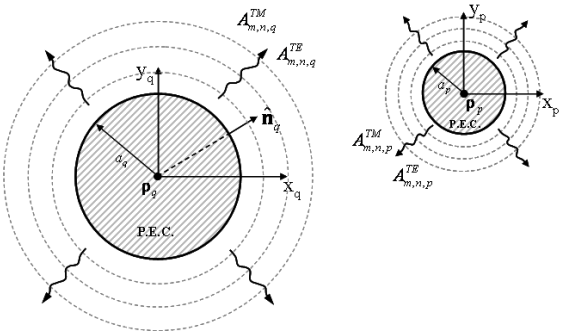


**Fig. 3.** Cylindrical wave-vectors expansion of the scattered fields by the perfect conducting cylinders.

## *2. Efficient analysis of SIW pillbox antennas*

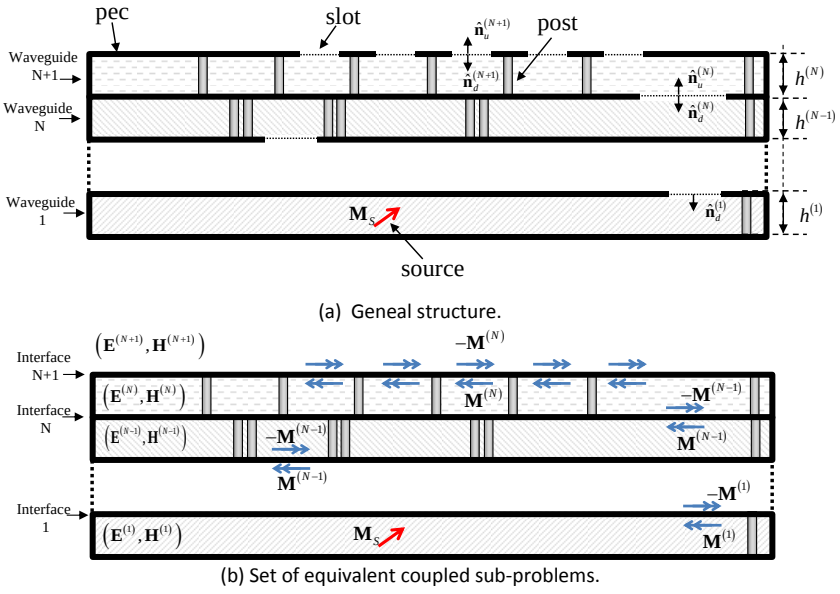


(a) Geneal structure.

(b) Set of equivalent coupled sub-problems.

**Fig. 4.** Topology of an SIW pillbox antennas realized on *N* dielectric substrates with its physical dimensions.

A pillbox antenna basically consists of a certain number *N* of stacked Parallel Plate Waveguides (PPW) on which via holes and slots are etched in order to realize waveguide channels, quasi-optical transitions between the different layers, and the radiating part [Fig. 4(a)].

By applying the equivalence principle to the PPW interface surfaces it is possible to fill the apertures on the generic *k*-th interface with PEC by introducing magnetic current distributions in order to guarantee the continuity of the electromagnetic field [Fig. 4(b)]

$$\begin{cases} \hat{\mathbf{n}}_d^{(k)} \times \mathbf{E}^{(k-1)} = \hat{\mathbf{n}}_u^{(k)} \times \mathbf{E}^{(k)} & (8.a) \\ \hat{\mathbf{n}}_d \times \mathbf{H}^{(k-1)} = \hat{\mathbf{n}}_u^{(k)} \times \mathbf{H}^{(k)} & (8.b) \end{cases}.$$

Boundary condition (8.a) is satisfied imposing

$$\hat{\mathbf{n}}_u^{(k)} \times \mathbf{E}_{k-1} = \mathbf{M}^{(k)} = -\mathbf{E}_k \times \hat{\mathbf{n}}_{k,u} = -\mathbf{M}^{(k)} \tag{9}$$

while condition (8.b) leads to

$$\hat{\mathbf{n}}_u^{(k)} \times \left\{ \mathbf{L}^{(k-1)} \left[ \mathbf{M}^{(k)}(\mathbf{r}') - \mathbf{M}^{(k-1)}(\mathbf{r}') \right] + \mathbf{H}_{inc}^{(k-1)} \right\} = \hat{\mathbf{n}}_u^{(k)} \times \left\{ \mathbf{L}^{(k)} \left[ \mathbf{M}^{(k+1)}(\mathbf{r}') - \mathbf{M}^{(k)}(\mathbf{r}') \right] + \mathbf{H}_{inc}^{(k)} \right\} \tag{10}$$

where the $\mathbf{L}$ operator is defined as:

$$\begin{aligned} \mathbf{L}^{(k)}[\mathbf{f}] \triangleq & -j\omega\varepsilon_k \int_{S_M} \underline{\underline{\mathbf{G}}}_{PPW}^{(k)}(\mathbf{r},\mathbf{r}') \cdot \mathbf{f} d\mathbf{r}' \\ & + \sum_{p=1}^{N_{post}^{(k)}} \sum_{m=1}^{+\infty} \sum_{n=-\infty}^{+\infty} A_{m,n,p}^{TM} \mathbf{M}_n\left(k_{\rho_m}^{(k)}, k_{z_m}^{(k)}, \boldsymbol{\rho} - \boldsymbol{\rho}_p, z\right) + A_{m,n,p}^{TE} \mathbf{N}_n\left(k_{\rho_m}^{(k)}, k_{z_m}^{(k)}, \boldsymbol{\rho} - \boldsymbol{\rho}_p, z\right) \end{aligned}. \tag{11}$$

Using the linearity properties of $\mathbf{L}$, (10) can be rewritten as

$$\hat{\mathbf{n}}_u^{(k)} \times \left\{ \mathbf{L}^{(k-1)} \left[ \mathbf{M}^{(k)}(\mathbf{r}') \right] - \mathbf{L}^{(k-1)} \left[ \mathbf{M}^{(k-1)}(\mathbf{r}') \right] - \mathbf{L}^{(k)} \left[ \mathbf{M}^{(k+1)}(\mathbf{r}') \right] + \mathbf{L}^{(k)} \left[ \mathbf{M}^{(k)}(\mathbf{r}') \right] \right\} = \hat{\mathbf{n}}_u^{(k)} \times \left\{ \mathbf{H}_{inc}^{(k)} - \mathbf{H}_{inc}^{(k-1)} \right\} \tag{12}$$

Eq. (12) can be solved adopting a Method of the Moment scheme. As first step, the generic current defined on the *k*-th interface has been expanded on the base $\left\{ \mathbf{b}_{f_k}^{(k)} \right\}$ as

$$\mathbf{M}^{(k)} = \sum_{f_k=1}^{N_k} v_{f_k}^{(k)} \mathbf{b}_{f_k}^{(k)}. \tag{13}$$

Next, using (13) in (12) and performing a Galerking testing procedure leads to a system of algebraic equations:

$$\sum_{f_k} v_{f_k}^{(k)} Y_{q_k,f_k}^{(k-1)} - \sum_{f_{k-1}} v_{f_{k-1}}^{(k-1)} Y_{q_k,f_{k-1}}^{(k-1)} - \sum_{f_{k+1}} v_{f_{k+1}}^{(k+1)} Y_{q_k,f_{k+1}}^{(k)} + \sum_{f_k} v_{f_k}^{(k)} Y_{q_k,f_k}^{(k)} = \left\langle \mathbf{b}_q^{(k)}, \left\{ \mathbf{H}_{inc}^{(k)} - \mathbf{H}_{inc}^{(k-1)} \right\} \right\rangle, \quad q = 1, \ldots N_{(k)} \tag{14}$$

where $Y_{q_k,f_k}^{(k)} = \left\langle \mathbf{b}_{q_k}^{(k)}, \mathbf{L}^{(k)} \left[ \mathbf{b}_{f_k}^{(k)} \right] \right\rangle$, and $\langle \, . \, , \, . \, \rangle$ denote the usual $L^2$ inner product.

The equation system (14) can be cast to the matrix form

$$
\begin{bmatrix}
\left(\underline{\underline{\mathbf{Y}}}^{(0)}_{q_1,f_1}+\underline{\underline{\mathbf{Y}}}^{(1)}_{q_1,f_1}\right) & -\underline{\underline{\mathbf{Y}}}^{(1)}_{q_1,f_2} & \underline{\underline{\mathbf{0}}} & \cdots & & & \underline{\underline{\mathbf{0}}} \\
-\underline{\underline{\mathbf{Y}}}^{(1)}_{q_2,f_1} & \left(\underline{\underline{\mathbf{Y}}}^{(1)}_{q_2,f_2}+\underline{\underline{\mathbf{Y}}}^{(2)}_{q_2,f_2}\right) & -\underline{\underline{\mathbf{Y}}}^{(2)}_{q_2,f_3} & \underline{\underline{\mathbf{0}}} & \cdots & & \underline{\underline{\mathbf{0}}} \\
\underline{\underline{\mathbf{0}}} & -\underline{\underline{\mathbf{Y}}}^{(2)}_{q_3,f_2} & \left(\underline{\underline{\mathbf{Y}}}^{(2)}_{q_3,f_3}+\underline{\underline{\mathbf{Y}}}^{(3)}_{q_3,f_3}\right) & -\underline{\underline{\mathbf{Y}}}^{(3)}_{q_3,f_4} & \underline{\underline{\mathbf{0}}} & \cdots & \vdots \\
\vdots & & & & & & \\
\underline{\underline{\mathbf{0}}} & & \cdots & \underline{\underline{\mathbf{0}}} & -\underline{\underline{\mathbf{Y}}}^{(k-1)}_{q_k,f_{k-1}} & \left(\underline{\underline{\mathbf{Y}}}^{(k-1)}_{q_k,f_k}+\underline{\underline{\mathbf{Y}}}^{(k)}_{q_k,f_k}\right) & -\underline{\underline{\mathbf{Y}}}^{(k)}_{q_k,f_{k+1}} & \underline{\underline{\mathbf{0}}} & \cdots & \underline{\underline{\mathbf{0}}} \\
\vdots & & & & & & \\
\underline{\underline{\mathbf{0}}} & \cdots & & & \cdots & \underline{\underline{\mathbf{0}}} & -\underline{\underline{\mathbf{Y}}}^{(m-1)}_{q_m,f_{m-1}} & \left(\underline{\underline{\mathbf{Y}}}^{(m-1)}_{q_m,f_m}+\underline{\underline{\mathbf{Y}}}^{(m)}_{q_m,f_m}\right) & -\underline{\underline{\mathbf{Y}}}^{(m)}_{q_m,f_{m+1}} \\
\underline{\underline{\mathbf{0}}} & \cdots & & & \cdots & \underline{\underline{\mathbf{0}}} & -\underline{\underline{\mathbf{Y}}}^{(m-1)}_{q_3,f_2} & \left(\underline{\underline{\mathbf{Y}}}^{(m)}_{q_{m+1},f_{m+1}}+\underline{\underline{\mathbf{Y}}}^{(m+1)}_{q_{m+1},f_{m+1}}\right)
\end{bmatrix}
\begin{bmatrix}
\mathbf{v}^{(1)} \\ \mathbf{v}^{(2)} \\ \mathbf{v}^{(3)} \\ \vdots \\ \\ \\ \vdots \\ \mathbf{v}^{(m)} \\ \mathbf{v}^{(m+1)}
\end{bmatrix}
=
\begin{bmatrix}
\mathbf{i}^{(1)} \\ \mathbf{i}^{(2)} \\ \mathbf{i}^{(3)} \\ \vdots \\ \\ \\ \vdots \\ \mathbf{i}^{(m)} \\ \mathbf{i}^{(m+1)}
\end{bmatrix}
\tag{15}
$$

Finally (15) can be solved using standard matrix approaches.

## Description of the main results obtained

The theory developed during the project has been implemented in a Matlab code.
As test case a pin-made slotted waveguide antenna has been considered. The structure is excited by a waveguide port as shown in Fig. 5, where all the dimensions and the substrate properties are labelled. The radiating part is composed of eight radiating slots preceded by a phase shifter. The phase shifter is realized using three air holes.
The equivalent magnetic current over each slot have been described using five entire domain basis functions.

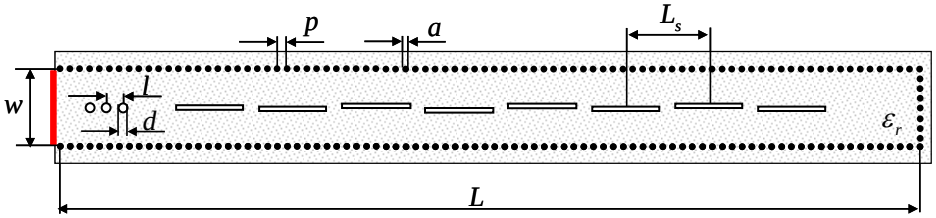


**Fig. 5.** Slotted waveguide antenna $\varepsilon_r$=2.2, $h$=0.508mm, $L$=66.4mm, $W$=5.76mm, $p$=0.8mm, $a$=4mm, $l$=0.8mm, $d$=0.4mm.

The input admittance obtained using this formulation and that obtained using the commercial software Ansys HFSS are reported in Fig.6, while a comparison of the radiated far-field in the H-plane at the frequencies of 24.15Ghz and 25.15Ghz is reported in Fig. 7.

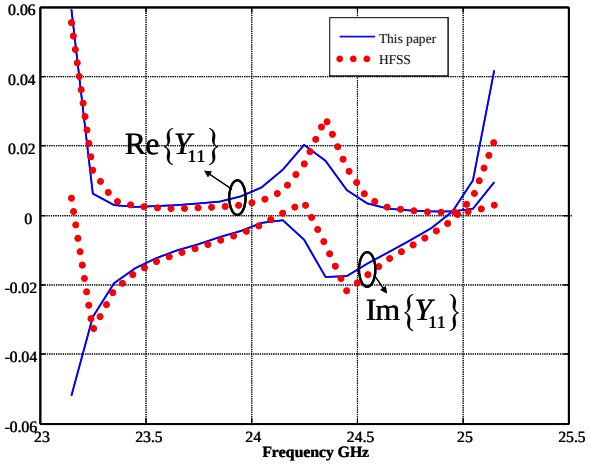


**Fig. 6.** Input admittance Y11 for the slotted waveguide antenna of Fig5 .

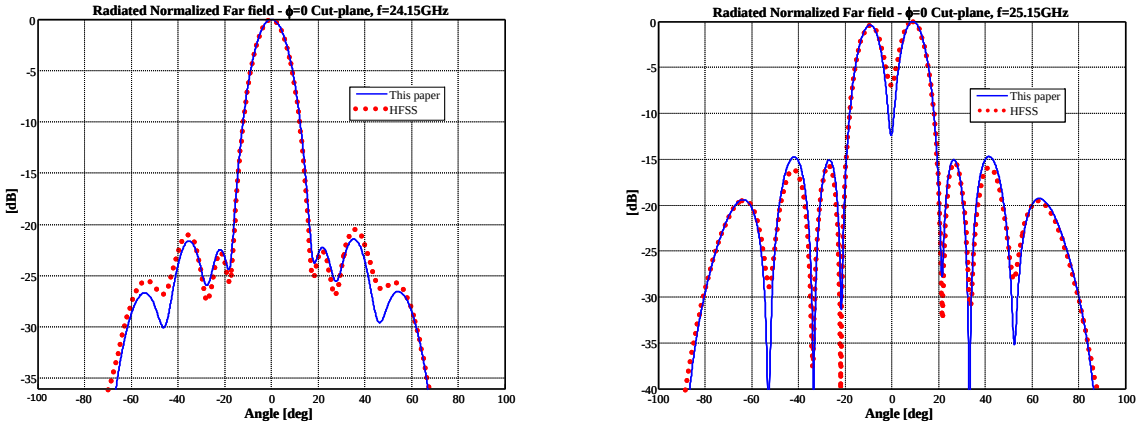


(a) (b)

**Fig. 7.** Far field radiated by a slotted (Fig. 14) in the H-plane at 24.15Ghz (a) and 25.15GHz (b).

The agreement between the full-wave simulation and the presented method is very good. We report in Tables I the CPU time and used memory for the simulation and compare them to those of Ansys HFSS$^{TM}$. The data have been generated using a Personal Computer with a 2.83GHz Intel Xeon E5440 CPU. These results demonstrate that the proposed algorithm is very efficient.

TABLE I

CPU SIMULATION TIME AND MEMORY USED ON A XEON E5540 2.83GHZ WITH 16GBYTE RAM

| METALLIC POSTS | DIELECTRIC POSTS | ANSYS HFSS | | | | THIS METHOD | |
|---|---|---|---|---|---|---|---|
| | | MESH | | ANALYSIS PER FREQUENCY | | | |
| | | TIME | MEMORY | TIME | MEMORY | TIME | MEMORY |
| 204 | 3 | 1782 s. | 1.8Gb | 286 s. | 1.8Gb | 74 s. | 70Mb |

## Project publications


[1] M. Casaletti, R. Sauleau, M. Ettorre and S. Maci, “Efficient Analysis of Metallic and Dielectric Posts in Parallel-Plate Waveguide Structures,” *IEEE Transactions on Microwave Theory and Techniques*, accepted.

[2] M. Casaletti, R. Sauleau, S. Maci, and M. Ettorre, "Mode matching method for the analysis of substrate integrated waveguides,” *6th European Conference on Antennas and Propagation (EUCAP)*, 2012, Prague.

[3] J. Seljan, M. Casaletti, G. Valerio, M. Ettorre, R. Sauleau, and S. Maci, “Novel Mode-Matching Technique for the Efficient Analysis of Complex Multi-Layer SIW and SISW-Based Structures”, *IEEE Symposium on Antenna and propagation (APS-URSI)*, 2012, Chicago.